Available online at www.sciencedirect.com
ScienceDirect
Journal of Catalysis 254 (2008) 383–396
JOURNAL OF CATALYSIS
www.elsevier.com/locate/jcat

Active sites in Fe/ZSM-5 for nitrous oxide decomposition and benzene hydroxylation with nitrous oxide

Keqiang Sun [a], Haian Xia [a], Zhaochi Feng [a], Rutger van Santen [b], Emiel Hensen [b,*], Can Li [a,*]

[a] State Key Laboratory of Catalysis, Dalian Institute of Chemical Physics, Chinese Academy of Sciences, Dalian 116023, China
[b] Schuit Institute of Catalysis, Eindhoven University of Technology, P.O. Box 513, 5600 MB Eindhoven, The Netherlands

Received 18 October 2007; revised 17 December 2007; accepted 16 January 2008

Available online 8 February 2008

Abstract

The effect of the iron content and the pretreatment conditions of Fe/ZSM-5 catalysts on the Fe speciation and the catalytic activities in nitrous oxide decomposition and benzene hydroxylation with nitrous oxide has been investigated. Iron-containing ZSM-5 zeolites with varying iron content (Fe/Al = 0.1–1.0) were prepared by solid-state ion exchange of HZSM-5 zeolite with $FeCl_3$ followed by hydrolysis and finally calcination at 823 K. In a second step, the catalysts were treated at 1173 K in He flow. The catalysts were characterized by FT-infrared, UV–vis and Raman spectroscopy. The number of Fe^{2+} centers was determined by low-temperature nitrous oxide decomposition and the subsequent methane titration. The highest activity for catalytic nitrous oxide decomposition was achieved for catalysts with intermediate iron loading (Fe/Al = 0.66). The activity after high-temperature treatment was about three times higher than after calcination. Whereas the calcined catalysts showed negligible activity in benzene hydroxylation, high-temperature treatment resulted in dramatic improvements in activity and selectivity. The selectivity to phenol decreased strongly with increasing Fe content. The profound changes in catalytic reactivity are related to the changes in iron speciation upon high-temperature treatment. Besides considerable extraction of Al from framework positions, resonance Raman spectroscopy points to changes in the structure of the iron oxide species of low nuclearity. A useful model is the reconstruction of charge-compensating cationic iron species to iron species stabilized by extraframework Al species located in the zeolite micropores. Further analysis of spectroscopic data suggests that oligonuclear, perhaps binuclear, iron sites appear most favorable for nitrous oxide decomposition, whereas the mononuclear iron sites are active for benzene hydroxylation to phenol.

Keywords: Zeolite; ZSM-5; Iron; Raman and infrared spectroscopy; Nitrous oxide decomposition; Benzene hydroxylation

1. Introduction

Fe-containing ZSM-5 catalysts are promising for a variety of environmentally-benign reactions [1–20]. Fe/ZSM-5 is reported to be highly active and stable in the decomposition of nitrous oxide which is useful to remove this potent greenhouse gas from the tail-gases of nitric acid plants [1–3]. Fe/ZSM-5 catalysts also catalyze the one-step hydroxylation of benzene to phenol with nitrous oxide as oxidant, providing a potential environmentally friendly alternative to the commonly used three-step process via cumene [4–14]. Other applications include selective catalytic reduction of NO_x with hydrocarbons or ammonia [15–18], oxidative dehydrogenation of alkanes [19] and selective oxidation of NH_3 to N_2 [20].

A major challenge to understand the catalytic activity of Fe/ZSM-5 catalysts lies in the heterogeneous distribution of the iron species. Extraframework Fe species stabilized in the zeolite micropores can be present as mono-, binuclear or oligonuclear cationic species, neutral iron oxide species with a varying degree of agglomeration and mixed oxide phases combining Fe and Al, while also bulk iron oxides on the external surface of the zeolite exist [6,13,21–35]. The exact preparation and pretreatment methods strongly affect the iron distribution. A large number of studies have attempted to assign the active site for the title reactions [4–17,21–41]. High-temperature treatment or steaming increases catalytic activity in nitrous oxide decompo-

* Corresponding authors. Faxes: +31 40 2455054, +86 411 84694447.
E-mail addresses: e.j.m.hensen@tue.nl (E. Hensen), canli@dicp.ac.cn (C. Li).

0021-9517/$ – see front matter
doi:10.1016/j.jcat.2008.01.017

sition and benzene oxidation substantially [2–14,21,25,36,42]. Besides Fe as an active component, others have stressed the role of Brønsted and Lewis acidity [43–47]. We have found indications that the active sites are formed by a combination of extraframework Fe and Al [10–12,36]. Panov has found evidence that the activity is related to the formation of a specific iron site denoted *α-site* [4,41] which leads via oxidation of active ferrous centers by nitrous oxide to the formation of reactive oxygen species (*α-oxygen*). Such oxygen species were proposed to be involved in the catalytic hydroxylation of benzene with nitrous oxide at higher temperatures (573–723 K) [4,41]. The linear correlation between the concentration of the α-sites and the rate of nitrous oxide decomposition [48] lends credence to the thought that the sites are also involved in catalytic N_2O decomposition. These observations suggest that the active sites for benzene oxidation and catalytic nitrous oxide decomposition are the same. However, this interpretation begins to be challenged by several recent studies. Based on the results that the turn-over frequency of the reaction of benzene to phenol decreases with increasing iron loading, Sachtler and co-workers [6,7] and Kiwi-Minsker and co-workers [9] have proposed that a mononuclear iron site is responsible for benzene hydroxylation. On the other hand, studies of catalytic nitrous oxide decomposition suggest that some clustering of iron species is more favorable [12,25].

Recently, we have carefully compared the iron speciation and activity of catalysts prepared from isomorphously substituted ZSM-5 zeolites with relatively low Fe loading (below 0.6 wt%) [12]. Here, catalysts with higher Fe loading in the range of 0.37–3.7 wt% (Fe/Al ratios of 0.11–1.0) prepared via solid-state ion exchange of dehydrated HZSM-5 zeolite with $FeCl_3$ are studied to compare the influence of the degree of iron clustering. The effect of high-temperature treatment is also investigated by comparing catalysts calcined in O_2 at 823 K or treated in He at 1173 K. The catalysts are characterized by infrared, UV–vis and Raman spectroscopy and the α-site density is determined. The catalytic activities in nitrous oxide decomposition and benzene hydroxylation by nitrous oxide are determined and the nature of the active site are discussed.

2. Experimental

2.1. Preparation of catalysts

Fe/ZSM-5 catalysts with varying iron loading were prepared by solid-state ion exchange [44,49]. Typically, two grams of NH_4ZSM-5 with a Si/Al ratio of 25 (NanKai University) was calcined in pure O_2 flow at 823 K and then grounded with an appropriate amount of $FeCl_3$ in an Ar-flushed glove box. The mixture was then heated in He flow from room temperature to 598 K at a rate of 8 K/min with an isothermal period at final temperature for 2 h. The resulted solid was subsequently treated in a flow of 0.5 vol% water in Ar from room temperature to 473 K to hydrolyse the Fe–Cl bonds. Finally, the material was calcined in flowing O_2 from room temperature to 823 K at a rate of 8 K/min and kept at the final temperature for 2 h to obtain Fe/ZSM-5(C,x), where C refers to the calcination in O_2 and x to the atomic ratio of Fe/Al. A portion of calcined Fe/ZSM-5(C,x) was further treated in He flow at 1173 K for 2 h and was denoted as Fe/ZSM-5(HT,x), where HT refers to high-temperature treatment.

2.2. Catalyst characterization

Infrared spectra were collected on a Nicolet Impact 410 FT-IR spectrometer in transmission mode with a DTGS detector at a resolution of 2 cm^{-1}. The samples were pressed into self-supporting wafers (∼15 mg/cm^2) and placed in a quartz cell sealed with NaCl windows. Prior to data collection, the calcined or high-temperature treated catalysts were treated in a flow of O_2 or N_2 at 773 K for 1 h, respectively. The sample was then cooled to room temperature in the same flow, followed by a nitrogen purge for 20 min. A reference spectrum was then collected. Subsequently, the sample was exposed to 1 vol% NO in He at a flow rate of 60 ml/min for 10 min and then purged with N_2 at a flow-rate of 60 ml/min for 10 min. Spectra were collected as a function of time of exposure to NO or N_2 purging. The overtones of the zeolite lattice vibrations in the reference spectra were used to normalize the spectra of the various samples.

UV–vis diffuse–reflectance spectra were recorded on a JASCO V-550 UV–vis spectrometer against $BaSO_4$ under ambient conditions. Resonance Raman spectra were recorded on a home-made Raman spectrometer with excitation lasers at 325 and 532 nm. The 325 nm and 532 nm laser lines are emitted from KIMMON IK-3351R-G He–Cd and Verdi-V10 (Coherent) lasers, respectively. An *in situ* cell was used to measure the Raman spectra under air-free conditions at room temperature. The acquisition time was varied between 10 and 120 min at a typical laser power of about 3 mW. There was no sample damage in view of the invariance of the spectra as a function of the acquisition time besides the signal-to-noise ratio. For the presented spectra acquisition times of 10–20 min were used.

Two methods were applied to determine the concentration of Fe^{2+} species (α-site). The first one is similar to the transient-response technique adopted by Kiwi-Minsker and co-workers [50]. The reactor effluent is continuously monitored after a step change of the carrier gas flow from a pure He to one containing nitrous oxide at 523 K: the decomposition of nitrous oxide at low temperatures will lead to gaseous N_2 concomitant with the deposition of an equal amount of α-oxygen species [41,48,50]. Quantification of the amount of molecular nitrogen evolved is used to determine the concentration of α-site based on the assumption that one oxygen atom is deposited per α-site [5,48]. Typically, an amount of 50 mg of catalyst was used for the determination of the concentration of α-sites. Prior to each run, the catalyst was treated in He at 823 K (for calcined catalysts) and at 1173 K for 2 h (for catalysts treated at high temperature) followed by cooling to 523 K in He. Subsequently, a step change was applied in the concentration of nitrous oxide from 0 to 5 vol% N_2O. A complementary method was used by determining the amount of deposited oxygen species via their reaction with methane. To this end, consecutive pulses of 0.23 ml 10 vol% CH_4 in He were administrated at 373 K to

the catalyst with deposited oxygen. It was assumed that one methane molecular reacts with two oxygen species to form adsorbed methoxy and hydroxyl groups [51].

2.3. Activity measurements

For catalytic nitrous oxide decomposition, a single-pass atmospheric quartz reactor with an inner diameter of 4 mm was used. A bed composed of 50 mg catalyst was held between two quartz wool plugs. The feed was 5 vol% N_2O in He at a GHSV of 24,000 h^{-1}. An on-line mass spectrometer (Gam 200, Pfeiffer Vacuum) calibrated by gases of known composition was used for quantitative analysis of gas-phase concentrations.

For benzene oxidation with nitrous oxide, a similar single-pass atmospheric quartz reactor system was used. Details of the reaction set-up have been described by Hensen et al. [8]. The feed consisted of a mixture of 1 vol% benzene and 4 vol% N_2O in He flow. A total flow rate of 100 ml/min was maintained at a total GHSV of 30,000 h^{-1}. A combination of online gas chromatography (HP 5890 column with FID detection, HP-5) and mass spectrometry (Balzers TPG 215) was used for quantification of gas-phase concentrations of reactants and products.

3. Results

3.1. Characterization

Fig. 1 displays the hydroxyl stretching region of the infrared spectra of the various Fe/ZSM-5 catalysts. The calcined materials exhibit a strong band at 3610 cm^{-1} due to the Brønsted acid hydroxyl groups and a weak band at 3740 cm^{-1} related to the silanol groups. With increasing iron content the band at 3740 cm^{-1} remains unchanged, while the intensity of the band at 3610 cm^{-1} decreases gradually. This latter trends tallies with the replacement of Brønsted acid sites by cationic Fe species from the solid-state exchange with $FeCl_3$. Treatment of the catalysts in flowing He at 1173 K leads to the complete disappearance of the band at 3610 cm^{-1}. Rehydration of these materials results in the appearance of a new band around 3670 cm^{-1} (not shown) due to the hydroxyl groups associated with aluminum at extraframework positions [52]. These results strongly suggest that the high-temperature treatment of the Fe/ZSM-5 catalysts results in the extensive extraction of the framework aluminum to extraframework positions.

Fig. 2 (left) shows the infrared spectra of NO adsorbed on the calcined Fe/ZSM-5 as a function of iron content. A small band around 1880 cm^{-1} is observed in the spectrum of Fe/ZSM-5 (C,0.11). With increasing Fe content, the band at 1880 cm^{-1} gradually grows together with the development of weak shoulders at 1858, 1912 and 1812 cm^{-1}. These features resemble those of NO adsorption on Fe/ZSM-5 with a relatively high iron loading prepared by chemical vapor deposition or solid-state ion exchange [23,32,53]. The bands at 1880 and 1858 cm^{-1} are generally assigned to mono-nitrosyl coordinating to Fe ions located in five- and six-membered rings of ZSM-5, respectively [23,31,53]. The bands at 1912 and 1812 cm^{-1}, observed when the Fe/Al ratio exceeds 0.33, are assigned to poly-nitrosyl

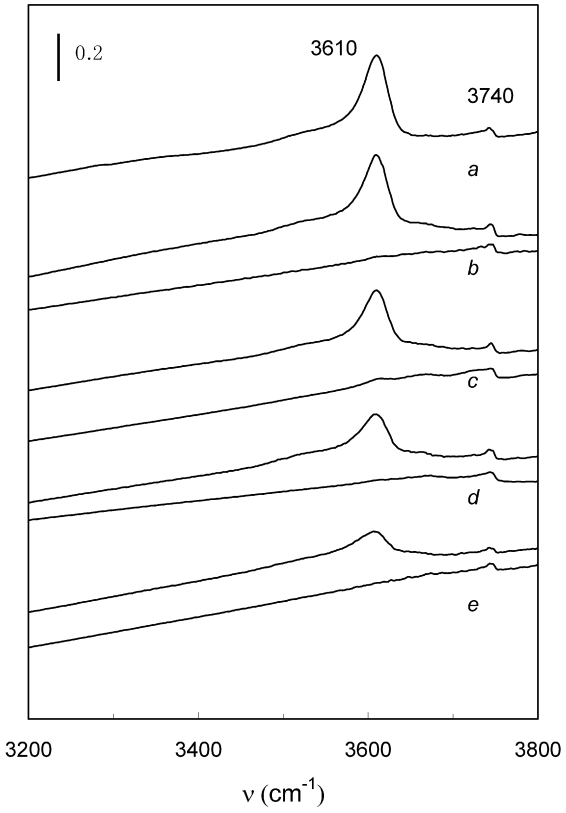

Fig. 1. Infrared spectra of the hydroxyl-stretching region: (a) H-ZSM-5, (b) Fe/ZSM-5(0.11), (c) Fe/ZSM-5(0.33) and (d) Fe/ZSM-5(0.66), (e) Fe/ZSM-5(1.0). The spectra of calcined (upper graph) and high-temperature treated (lower graph) samples (b–e) are shown.

groups on isolated Fe^{2+} sites [23,31,32,53,54]. Fig. 2 (right) shows the effect of nitrogen purging on the infrared spectra of adsorbed NO for calcined Fe/ZSM-5. After a purge of 10 min the mono-nitrosyl bands (1880, 1858 cm^{-1}) and poly-nitrosyl bands (1912, 1812 cm^{-1}) have almost completely disappeared and new bands at 1578, 1600, 1625 and 1645 cm^{-1} can be discerned for Fe/ZSM-5(C,0.11). With increasing iron loading the bands at 1625, 1600 and 1578 cm^{-1} grow. The band at 1645 cm^{-1} was assigned to NO_2 on structural defects of the zeolite for steamed Fe/ZSM-5 [12,38]. The bands at 1600 and 1625 cm^{-1} have been well-documented and attributed to NO_2 on iron-oxide species resulting from purging after NO adsorption and the band at 1578 cm^{-1} is generally assigned to nitrate groups [12,31,32,53]. The reason for the appearance of such NO_2 bands remains moot. One explanation could be that some oxidation of NO to NO_2 occurs, perhaps with residual oxygen or extraframework oxygen, which apparently only adsorbs after lowering the NO surface coverage during purging. One also should not exclude the possibility of very small amounts of NO_2 in the NO probe gas. The infrared spectra of NO adsorbed on Fe/ZSM-5(HT,0.11) (Fig. 3a) show a band at 1874 cm^{-1} with a shoulder at 1890 cm^{-1}. The intensities of these bands increase also with iron loading. For Fe/ZSM-5 with Fe/Al ratios close to 0.66, weak absorption bands at 1912 and 1812 cm^{-1} due to poly-nitrosyl groups on isolated Fe^{2+} site are observed. Fig. 3 (right) shows the effect of nitrogen purging on these spectra. The bands of poly-nitrosyl groups disappear

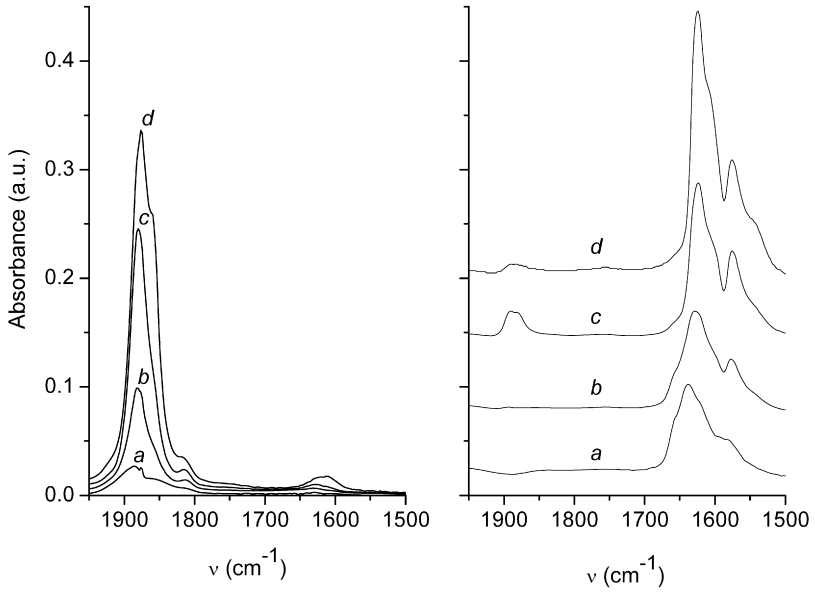

Fig. 2. Infrared spectra of adsorbed NO of (left) calcined Fe/ZSM-5 and (right) after N_2 purging for 10 min: (a) Fe/ZSM-5(C,0.11), (b) Fe/ZSM-5(C,0.33), (c) Fe/ZSM-5(C,0.66) and (d) Fe/ZSM-5(C,1.0).

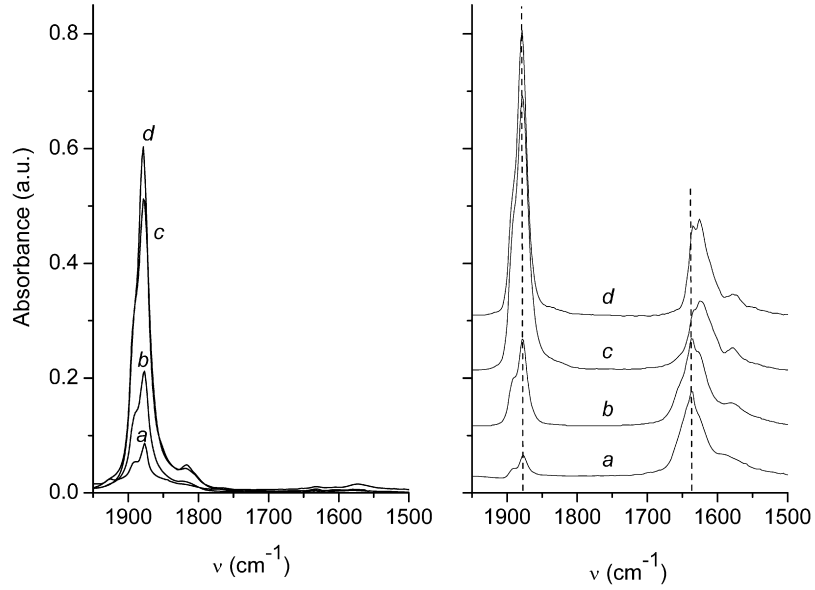

Fig. 3. Infrared spectra of adsorbed NO of (left) high-temperature treated Fe/ZSM-5 and (right) after N_2 purging for 10 min (indicated are the bands at 1874 and 1635 cm^{-1}: (a) Fe/ZSM-5(HT,0.11), (b) Fe/ZSM-5(HT,0.33), (c) Fe/ZSM-5(HT,0.66) and (d) Fe/ZSM-5(HT,1.0).

completely whereas the bands at 1874 and 1890 cm^{-1} attenuate only slightly. Furthermore, a new band at 1636 cm^{-1} appears as well as the bands of nitro and nitrate groups at 1625 and 1578 cm^{-1} with reduced intensities as compared to the corresponding calcined catalysts. These differences indicate that extensive restructuring of the iron oxide phase has occurred during the high-temperature treatment.

A doublet at 1874 and 1892 cm^{-1} has been earlier reported by Mul et al. on a steamed [FeAl]MFI prepared by isomorphous substitution [31]. These bands showed a similar dynamic behavior upon purging. Replacement of Al by Ga shifted the doublet to 1867 and 1881 cm^{-1} without changing their relative intensities. However, different assignments of these bands exist: the strong band at 1874 cm^{-1} was related to NO adsorption on mixed oxide $FeAlO_x$ and the shoulder band at 1892 cm^{-1} to mono-nitrosyl on isolated iron or oligonuclear iron species. In the present study, the doublet was not observed on the calcined samples and was only found in the high-temperature treated Fe/ZSM-5 catalysts. The relative intensity ratio between the band at 1874 cm^{-1} and the one at 1890 cm^{-1} remains unchanged irrespective of the iron content. We cannot conclude firmly on the nature of the species causing such bands and whether they are due to one or two Fe species. A reasonable explanation is linked to the migration of Al. Thus, the band at 1874 cm^{-1} could be related to NO adsorbed Fe–O–Al species since the band was absent in the calcined catalysts. The band

at 1890 cm^{-1} may have shifted from its initial position at 1880 cm^{-1} due to modifications to the zeolite framework which influences the Fe ions.

In the region around 1600 cm^{-1}, the band at 1636 cm^{-1} has been suggested to be a NO_2 group coordinating to an extraframework mixed oxide $FeAlO_x$ by Mul et al. [31] or similarly Fe–O–Al species by Hensen et al. [10–12]. The observation of this band is in line with the tentative assignment of the band at 1874 cm^{-1} to aluminum-containing iron oxo species as a result of extensive extraction of framework Al to extraframework positions upon high-temperature treatment. We deconvoluted the IR spectra after purging with the weakly adsorbed NO removed and plotted in Fig. 4 the intensity of various bands as a function of the Fe/Al ratio. One notes that the areas of the related bands at 1874 and 1892 cm^{-1} go through a maximum at a Fe/Al ratio of 0.66, whereas that of the band at 1636 cm^{-1} decreases with increasing iron loading. This observation suggests that different aluminum-containing iron-oxo species exist in Fe/ZSM-5(HT,x) or alternatively that a certain fraction of such species gives rise to the 1635 cm^{-1} band.

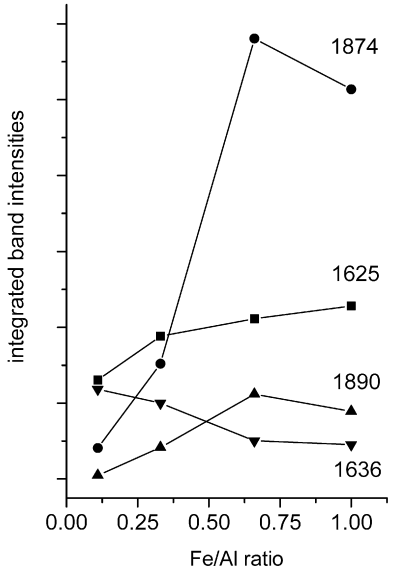

Fig. 4. Intensity of the infrared bands after room-temperature NO adsorption followed by purging with N_2 for 10 min as a function of iron loading on Fe/ZSM-5(HT,x).

Fig. 5 shows the diffuse–reflectance UV–vis spectra of the Fe/ZSM-5 catalysts. For the calcined catalysts (Fig. 5, left), two intense charge transfer bands at 240 and 355 nm are observed for Fe/ZSM-5(C,0.11). The intensities of the two bands increase with the iron content. Similarly, the ratio of the intensities of the band at 355 nm relative to the one at 240 nm increases. Additionally, a new band around 550 nm becomes pronounced at Fe/Al $\geqslant$ 0.66. Finally, the spectrum of Fe/ZSM-5 (C,1.0) is dominated by strong and broad features at 350 and 550 nm. These changes with iron loading are in accord with the changes in the visual appearance of the calcined catalysts ranging from white/yellow (low iron loading) to brown (high iron loading). The bands below 300 nm are typical LMCT bands of isolated Fe^{3+} species either tetrahedrally or octahedrally coordinated [29,30,55,56]. At higher wavelengths one distinguishes bands around 280 nm for isolated octahedral Fe^{3+} complexes, around 350 nm for octahedral Fe^{3+} in oligomeric clusters and above 400 nm for bulky Fe_2O_3-like aggregates [22,29,30,55,56]. A recent detailed analysis [57] further revealed that iron dimers also have UV–vis adsorption below 300 nm without the appearance of bands at around 350 nm. The present UV–vis spectra indicate that the calcined materials contain a distribution of iron species ranging from isolated ions to bulky iron oxide agglomerates. Clearly, more extensive clustering takes place with increasing Fe loading. Further treatment of the Fe/ZSM-5 samples at 1173 K in He flow results in substantial changes of the UV–vis spectra (Fig. 5, right). The intensities of the bands at 240 and 355 nm, due to the isolated and clustered iron-oxo

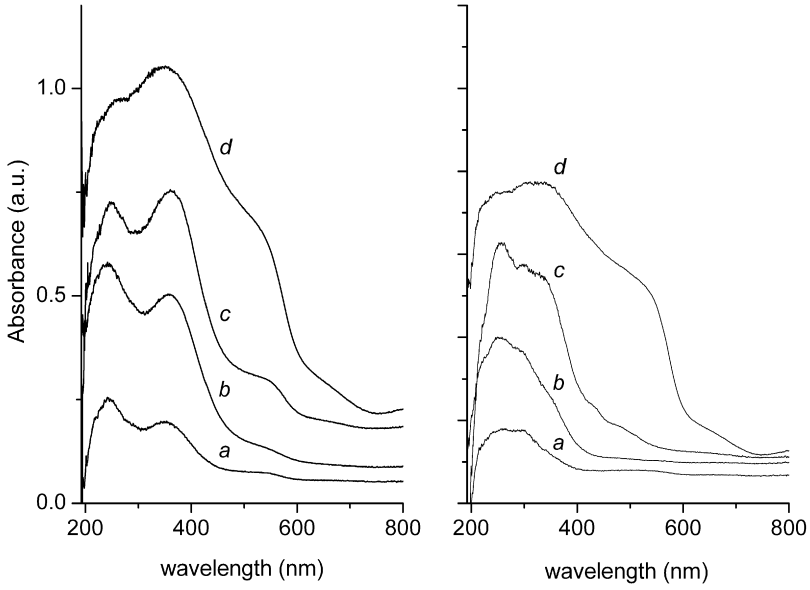

Fig. 5. Diffuse–reflectance UV–vis spectra of (left) calcined Fe/ZSM-5 and (right) high-temperature treated Fe/ZSM-5: (a) Fe/ZSM-5(0.11), (b) Fe/ZSM-5(0.33), (c) Fe/ZSM-5(0.66) and (d) Fe/ZSM-5(1.0).

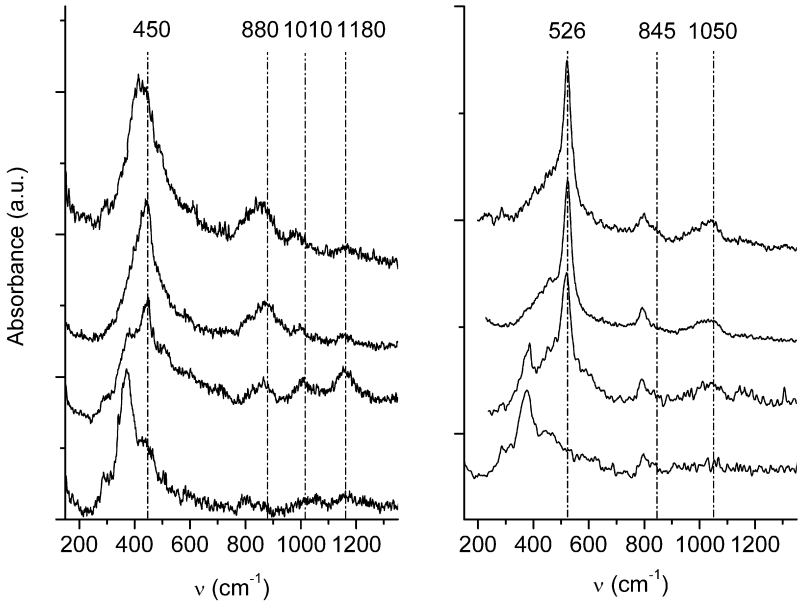

Fig. 6. Raman spectra with excitation at 325 nm of (left) calcined Fe/ZSM-5 and (right) high-temperature treated Fe/ZSM-5: (a) Fe/ZSM-5(0.11), (b) Fe/ZSM-5 (0.33), (c) Fe/ZSM-5(0.66) and (d) Fe/ZSM-5(1.0).

species, respectively, are substantially reduced. A new band at 290 nm can be discerned and its intensity increases with the iron content. This band has been reported earlier for a steamed iron-containing ZSM-5 catalyst [29] and a similar band at 286 nm has also been assigned to Fe^{3+} in octahedral coordination in Al_2O_3 [30]. Thus, the band at 290 nm could be assigned to octahedral ferric ions in close interaction with Al species. The dramatic changes of the optical spectra after high-temperature treatment point to profound changes in the iron speciation.

Fig. 6 (left) shows the Raman spectra of the calcined catalysts when an excitation line of 325 nm was used. Besides the bands at 380 and 800 cm^{-1} that are characteristic for zeolite MFI [33,58], weak bands at 455, 880, 1010 and 1180 cm^{-1} are observed for Fe/ZSM-5(C,0.11). The intensities of the latter four bands increase for Fe/ZSM-5(C,0.33). Simultaneously the bands related to MFI decrease. XRD (not shown) indicates that the structure is not damaged. The reason for the decrease of the MFI-related vibrational bands can be partially attributed to the perturbation of the zeolite vibrations by the presence of extraframework Fe species. On the other hand, the Fe/Si ratio of this set of samples quite low. Another explanation for this behavior relates to the scattering nature of Raman spectroscopy which makes it a surface-sensitive technique. With higher iron content, the color change of the samples (*vide infra*) may lead to partial masking of the zeolite-related signals. A further increase in iron loading results in the intensification of the bands around 455 and 880 cm^{-1}, whereas the intensities of the bands at 1010 and 1180 cm^{-1} are reduced. For Fe/ZSM-5(C,1.0), a band shift from 455 to 430 cm^{-1} is observed, while a weak feature at 610 cm^{-1} can also be discerned. These latter two vibrations are related to the formation of more bulky Fe_2O_3 aggregates [59]. The bands around 1100 cm^{-1} are typically asymmetric stretching vibrations of isolated TM–O–Si entities with TM being a transition metal ion either in the framework or at extraframework positions [33,58,60,61]. Accordingly, the bands at 1010 and 1180 cm^{-1} are ascribed to isolated iron cations grafted at different positions of the ZSM-5 structure. The bands around 455 and 880 cm^{-1} are assigned to clustered iron species because their intensities increase with the iron loading. Spectroscopic studies of binuclear iron-oxo complexes have revealed that the symmetric stretching frequency of an Fe–O–Fe cluster lies between 380–540 cm^{-1} and the asymmetric stretching frequency between 725–885 cm^{-1}, the exact frequency depending on the angle of the Fe–O–Fe entity [62,63]. A strong indication that these bands in the Fe/ZSM-5 catalysts relate to Fe species of low nuclearity is the finding that the intensities of the bands is strongly reduced when a 532 nm laser line is used to excite the catalyst. Accordingly, the bands around 455 and 880 cm^{-1} are tentatively assigned to a binuclear iron-oxo clusters with an Fe–O–Fe angle of about 150°. These binuclear sites may be present as such or be part of some iron oxide phase of low Fe nuclearity.

Fig. 6 (right) shows the Raman spectra of the catalysts treated at 1173 K in He using an excitation line at 325 nm. Only the bands at 380 and 800 cm^{-1}, assigned to the zeolite ZSM-5 structural vibrations, can be clearly observed in the spectrum of the Fe/ZSM-5(HT,0.11). Three new bands at 526, 845 and 1050 cm^{-1} are observed for catalysts with higher Fe loading. According to the above assignment and those in the literature [33,58], the bands at 526 and 845 cm^{-1} could be attributed to the symmetric and asymmetric stretching vibrations of a Fe–O–Fe cluster of low nuclearity, and the bands at 1050 cm^{-1} to the stretching vibration of a new isolated iron species, respectively. Note that the band at 845 cm^{-1} is extremely weak and appears as a shoulder to the zeolite vibration at 800 cm^{-1}. Similar to the case for the calcined samples, when the Raman spectra were collected using excitation at 532 nm, the intensity of the band at 526 cm^{-1} ascribed to the symmetric stretching

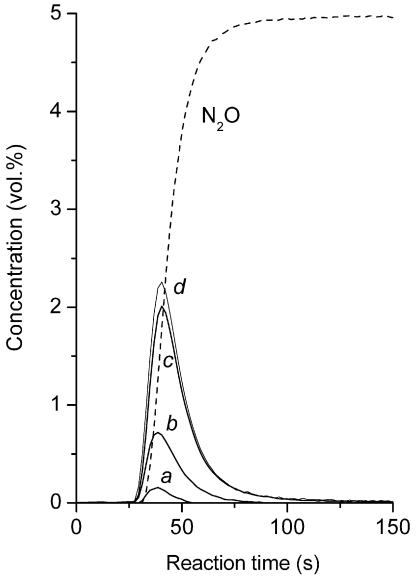

Fig. 7. Response to a step change from He flow to 5 vol% N_2O in He flow for Fe/ZSM-5(HT,x): (a) Fe/ZSM-5(HT,0.11), (b) Fe/ZSM-5(HT,0.33), (c) Fe/ZSM-5(HT,0.66) and (d) Fe/ZSM-5(HT,1.0). The dashed line represents the N_2O concentration.

vibration of the Fe–O–Fe species is decreased strongly. This effect is related to resonance and pre-resonance enhancement Raman effects since excitation at 325 nm is close to the absorption bands of oligonuclear Fe species (355 nm) and of an Fe species in close interaction with extraframework aluminum (290 nm). The dependence of the stretching frequency of the Fe–O–Fe entity on the Fe–O–Fe angle [62,63] then suggests that the shift of the band position of 455 cm^{-1} for the calcined catalyst to 526 cm^{-1} for the high-temperature treated catalyst is related to a change of the Fe–O–Fe angle from ∼150° to ∼130°. The important point to conclude here is that considerable reconstruction of oligonuclear Fe sites takes place as a consequence of the high-temperature treatment. Moreover, this treatment also shifts the bands of mononuclear Fe species at 1010 and 1180 cm^{-1} in the calcined catalyst to 1050 cm^{-1} and here it also appears that high-temperature calcination modifies the structure around such isolated sites.

3.2. Concentration of active Fe centers

The number of active Fe centers (α-sites) was determined by nitrous oxide decomposition at 523 K. Fig. 7 shows the response to a step change from a flow of He to 5 vol% N_2O in He over the Fe/ZSM-5(HT,x) catalysts. Indeed, only N_2O and N_2 are observed in the reactor effluent. Therefore, surface oxygen $(O)_{ads}$ species must be formed. The number of the surface oxygen and the density of active centers can be quantified by measuring the amount of evolved molecular nitrogen. For Fe/ZSM-5(HT,x) with $x = 0.11$, 0.33, 0.66 and 1, the active site densities are 3.5×10^{18}, 2.5×10^{19}, 7.9×10^{19} and 8.9×10^{19} g^{-1}, corresponding to atomic oxygen to total Fe (O/Fe) ratios of 0.08, 0.20, 0.31 and 0.23, respectively. Similar experiments for the calcined catalysts revealed that the amount of nitrous oxide decomposed under these conditions is negligible. This agrees with the notion that severe treatment is a prerequisite to the formation of α-sites [4,48,50]. The amount of active surface oxygen was further determined by their titration with methane. One methane molecule reacts with two surface oxygen atoms to form an adsorbed methoxy and an hydroxyl group [51]. From the amount of consumed CH_4, the number of surface oxygen reactive towards CH_4 over Fe/ZSM-5(HT,x) with $x = 0.11$, 0.33, 0.66 and 1 were found to be 3.3×10^{18}, 2.1×10^{19}, 6.4×10^{19} and 4.5×10^{19} g^{-1}, corresponding to atomic O/Fe ratios of 0.079, 0.16, 0.24 and 0.12, respectively (Table 1). These values are slightly lower than those determined by N_2O decomposition at 523 K, which is in line with the observation that only a portion of the surface oxygen species deposited by N_2O decomposition are active in CO oxidation [50] or $^{18}O_2$ isotopic exchange [64]. Thus, the value obtained from methane titration yields the most accurate estimation of the number of α-sites. Fe/ZSM-5(HT,0.66) with a medium iron content is found to have the highest oxygen density as well as the highest O/Fe ratio.

Table 1
The concentration of Fe^{2+} (α-sites) determined by low-temperature N_2O decomposition at 523 K and CH_4 titration at 373 K for Fe/ZSM-5 after high-temperature treatment

Catalyst	N_2O decomposition		CH_4 titration	
	[O] (10^{18} atom/g)	O/Fe_{total}	[O] (10^{18} atom/g)	O/Fe_{total}
Fe/ZSM-5(HT,0.11)	3.5	0.08	3.3	0.08
Fe/ZSM-5(HT,0.33)	25.0	0.20	21.0	0.16
Fe/ZSM-5(HT,0.66)	79.0	0.31	52.0	0.20
Fe/ZSM-5(HT,1.0)	89.0	0.23	45.0	0.12

3.3. Catalytic decomposition of nitrous oxide

The conversion during catalytic nitrous oxide decomposition as a function of reaction temperature is shown in Fig. 8. The N_2O conversion increases with iron content for both the calcined and the high-temperature treated catalysts. High-temperature treatment significantly enhances the catalysts activity. The temperature required for 50% conversion for the Fe/ZSM-5(HT,x) catalysts are 20–30 K lower than those for the corresponding calcined counterparts, which is consistent with our previous results [36,42,65]. The apparent first-order reaction rates at 698 K expressed per mol Fe atom are shown in Fig. 9. For both the calcined and high-temperature treated catalysts, the highest rates are observed at the iron content of Fe/Al = 0.66, and the activity of Fe/ZSM-5(HT,0.66) is about three times higher than that of Fe/ZSM-5(C,0.66). Table 2 lists the apparent activation energies and the pre-exponential factors for the various catalysts on the basis of the apparent first-order reaction of N_2O decomposition. The apparent activation energy for Fe/ZSM-5(C,0.11) is around 180 kJ/mol, which is consistent with the value obtained by Bell and co-workers for the calcined Fe/ZSM-5 catalyst with a low iron content [66]. With increasing iron content the apparent activation energy decreases for the calcined catalysts and levels off at about 147 kJ/mol when the Fe/Al ratio exceeds 0.66, which agrees with reported

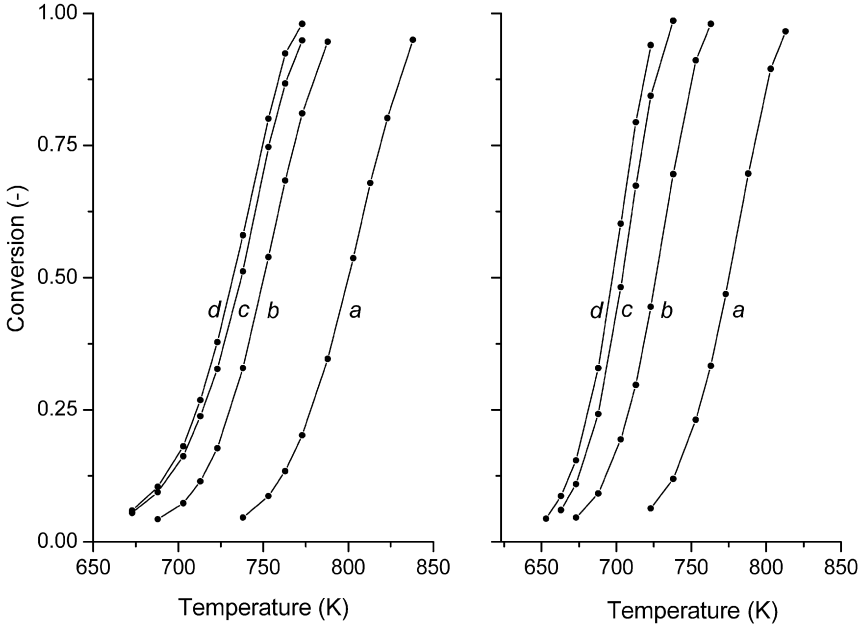

Fig. 8. Steady-state nitrous oxide conversion as a function of reaction temperature of (left) Fe/ZSM-5(C,x) and (right) Fe/ZSM-5(HT,x): (a) Fe/ZSM-5(0.11), (b) Fe/ZSM-5(0.33), (c) Fe/ZSM-5(0.66) and (d) Fe/ZSM-5(1.0). The feed consists of 5 vol% N_2O in He.

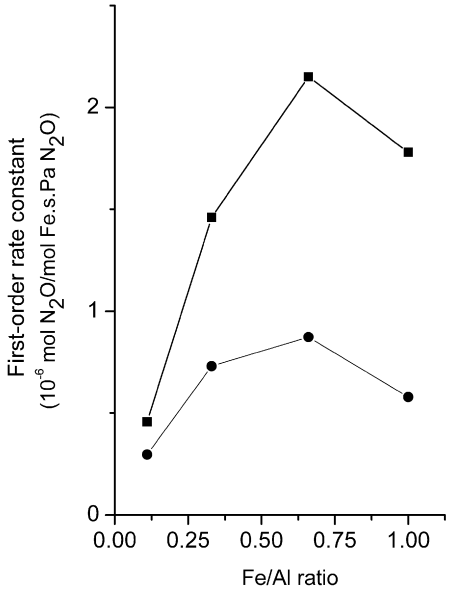

Fig. 9. Relation between the first-order reaction rate constant for catalytic nitrous oxide decomposition at 693 K and the iron loading for (●) calcined Fe/ZSM-5 and (■) high-temperature treated Fe/ZSM-5.

values (130–150 kJ/mol) for sublimed Fe/ZSM-5 with a Fe/Al ratio of about 1.0 [42,67]. On the other hand, the apparent activation energies for the high-temperature treated catalysts are all close to 190 kJ/mol, independent of the iron content. Such values have also been reported by Zhu et al. [27] and Bell and co-workers [68] for Fe/ZSM-5 after high-temperature treatment or steaming.

3.4. Benzene hydroxylation

The rate of phenol formation over various catalysts as a function of time on stream is shown in Fig. 10. Typically, a high initial rate is followed by gradual deactivation. The catalyst with the lowest iron content (Fe/Al = 0.11), either in the series of the calcined catalysts or the high-temperature treated ones, exhibits the highest rate of phenol formation. However, the calcined Fe/ZSM-5(C,x) catalysts showed rather low selectivities to phenol and instead substantial amounts of CO_x and H_2O were formed (Table 3) indicating an important contribution of deep benzene oxidation. This observation is in line with the work of Hensen and co-workers [8] for calcined Fe/ZSM-5. The activity and selectivity data of the calcined catalysts shown in Table 3 further reveal that both the conversions of benzene and nitrous oxide increase with the iron content, whereas the selectivities of benzene and nitrous oxide to phenol decrease monotonously with iron content. This indicates an increasing contribution of benzene combustion relative to the selective oxidation of benzene. High-temperature treatment of the calcined catalysts results in general in a twofold increase of the rate of phenol formation (Table 4). However, the phenol reaction rate decreases significantly with iron content with increasing contributions of combustion. A three-fold increase in iron content from Fe/Al = 0.11 to 0.33 brings about a four-fold decrease in the rate of phenol production. The rates are very low for Fe/ZSM-5(HT,0.66) and Fe/ZSM-5(HT,1.0). This observation is consistent with those of Sachtler and co-workers [6,7]. Although this treatment of Fe/ZSM-5 decreases substantially the N_2O conversion, the selectivities of benzene and N_2O to the product of selective oxidation are substantially increased after such treatment. For catalysts with Fe/Al ratios lower than 0.66, the selectivity of benzene is close to 99% and the selectivity of N_2O is above 70% after a reaction time of 1 h, which accounts for the higher rate of phenol formation for the catalysts after high-temperature treatment. With increasing iron loading, the selectivity of nitrous oxide decreases monotonously from about 85% for Fe/ZSM-5(HT,0.11) to 50% on Fe/ZSM-5

Table 2
Activation energies and pre-exponential factors for nitrous oxide decomposition

Catalyst	Fe (wt%)	Pretreatment	E_{act}[a] (kJ/mol)	A[b] (mol N_2O/s mol Fe Pa N_2O)	Ref.
Fe/ZSM-5(C.0.11)	0.4	823 K, O_2	184	3.1×10^7	This work
Fe/ZSM-5(C,0.33)	1.2	823 K, O_2	174	8.9×10^6	This work
Fe/ZSM-5(C,0.66)	2.4	823 K, O_2	148	1.3×10^5	This work
Fe/ZSM-5(C,1.00)	3.7	823 K, O_2	147	6.6×10^4	This work
Fe/ZSM-5(1.1)[c]	4.5	773 K, He	139	1.8×10^6	[62]
Fe/ZSM-5(0.97)	3.6	823 K, O_2	136	–	[42]
Fe/ZSM-5(HT,0.11)	0.4	1173 K, He	189	7.4×10^7	This work
Fe/ZSM-5(HT,0.33)	1.2	1173 K, He	189	2.3×10^8	This work
Fe/ZSM-5(HT,0.66)	2.4	1173 K, He	190	4.8×10^8	This work
Fe/ZSM-5(HT,1.00)	3.7	1173 K, He	188	2.6×10^8	This work
Fe/ZSM-5(0.97)	3.7	973 K, steaming	195	–	[42]
Fe/ZSM-5(0.38)[d]	0.38	1123 K, He	185	$9.9.10^8$	[10]

[a] Apparent activation energy.
[b] Pre-exponential factor.
[c] Pre-exponential factor calculated at 698 K.
[d] Fe/ZSM-5 is prepared by isomorphous substitution.

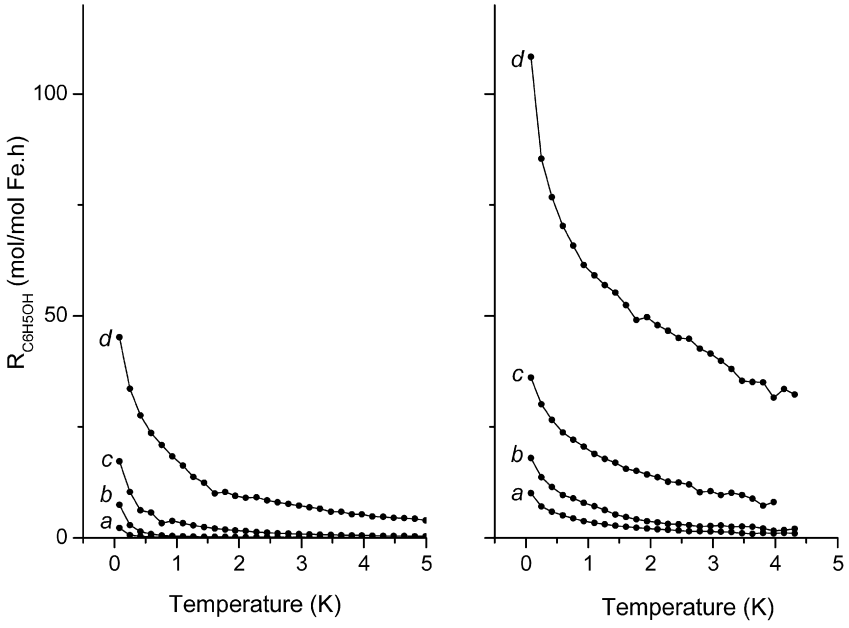

Fig. 10. Rate of phenol production at 623 K as a function of iron loading for (left) calcined Fe/ZSM-5 and (right) the high-temperature treated Fe/ZSM-5: (a) Fe/ZSM-5(0.11), (b) Fe/ZSM-5(0.33), (c) Fe/ZSM-5(0.66) and (d) Fe/ZSM-5(1.0).

(HT,1.0). The reason that the nitrous oxide selectivity is lower than the benzene selectivity is related to the fact that during the first hour of reaction considerable deposits are formed which are then slowly oxidized by nitrous oxide. This effect is more pronounced with higher Fe content. For catalysts with low Fe content, this effect was not observed except for an Fe loading of 0.45 wt% [12]. Note that an increase of the iron content results in a decrease of the benzene and nitrous oxide conversions.

4. Discussion

4.1. Reconstruction of iron species upon high-temperature treatment

Treating the calcined Fe/ZSM-5(C,x) in He at 1173 K drastically enhances the catalytic activity in the decomposition of nitrous oxide and the selective oxidation of benzene to phenol. The influence of such treatment on the nature of the iron sites is thus very relevant. For Fe/ZSM-5 calcined at 823 K, a distribution of mononuclear iron species, small oligonuclear iron clusters and bulk-like iron oxide aggregates follows from the UV–vis spectra. With increasing iron content, the relative amounts of oligonuclear iron clusters (350 nm) and bulky iron oxide aggregates (550 nm) increase. Infrared spectra reveal that part of the iron species is present at cationic exchange positions replacing the protons, while another part forms neutral iron oxide species. Infrared spectra of NO adsorption further identify three types of cationic iron species (Fig. 2). The cation-exchange position in the five-membered rings is first occupied at low iron content (band of mono-nitrosyl at 1880 cm^{-1}), followed by occupation of the exchange position

Table 3
Reaction data (X—conversion, S—selectivity) for benzene hydroxylation by calcined Fe/ZSM-5 catalysts

Catalysts	Time (h)	Benzene		Nitrous oxide		R_{phenol}[a]
		X	S	X	S	
Fe/ZSM-5(C,0.11)	1	7	74	2	51	1.3
	2	2	55	2	40	0.58
	4	2	53	1	25	0.38
Fe/ZSM-5(C,0.33)	1	7	42	11	7	0.78
	2	5	26	11	3	0.35
	4	5	9	13	1	0.12
Fe/ZSM-5(C,0.66)	1	12	6	38	1	0.19
	2	14	2	47	2	0.09
	4	14	2	50	<1	0.06
Fe/ZSM-5(C,1.00)	1	21	2	73	<1	0.12
	2	21	2	75	<1	0.09
	4	27	1	76	<1	0.06

[a] Reaction rate of phenol in mmol/(g h).

Table 4
Reaction data (X—conversion, S—selectivity) for benzene hydroxylation by high-temperature treated Fe/ZSM-5 catalysts

Catalysts	Time (h)	C_6H_6		N_2O		R_{phenol}[a]
		X	S	X	S	
Fe/ZSM-5(HT,0.11)	1	16	>99	5	81	4.35
	2	13	>99	4	85	3.52
	4	8	>99	3	87	2.24
Fe/ZSM-5(HT,0.33)	1	16	>99	6	68	4.24
	2	12	>99	4	74	2.95
	4	6	>99	3	76	1.67
Fe/ZSM-5(HT,0.66)	1	13	>99	5	65	3.34
	2	6	>99	3	60	1.59
	4	3	>99	2	47	0.69
Fe/ZSM-5(HT,1.00)	1	11	83	4	55	2.44
	2	7	73	2	52	1.37
	4	4	58	1	48	0.70

[a] Reaction rate of phenol in mmol/(g h).

in six-membered rings (1858 cm^{-1}) and ten-membered rings (poly-nitrosyl bands at 1912 and 1812 cm^{-1}) at higher iron loading.

Treatment of the catalysts in He at 1173 K leads to substantial changes in the iron speciation. UV–vis spectra show a more pronounced band at 290 nm tentatively assigned to isolated iron species associated with Al species, while the band at 350 nm related to oligonuclear iron clusters is reduced substantially. The substantial decrease of the number of bridging hydroxyl groups as determined by infrared spectra points to extensive dealumination of Fe/ZSM-5. This does not appear to depend on the iron loading. After high-temperature treatment, the infrared spectra of adsorbed NO reveal that the cationic iron species in the five- and six-membered rings (bands at 1882 and 1858 cm^{-1}) of the zeolite for the calcined Fe/ZSM-5 have been replaced by mixed iron and aluminum oxide species characterized by bands at 1874 cm^{-1}. The new band at 1635 cm^{-1} obtained after purging the catalysts (Fig. 3) is also related to such species.

More detailed insight is provided by resonance enhancement Raman spectroscopy. Excitation at 325 nm results in enhancement of the band intensities related to mono- and especially oligonuclear Fe species. An important finding is that the symmetric stretching frequency of Fe–O–Fe entities in such oligonuclear Fe species changes considerably upon high-temperature treatment of calcined Fe/ZSM-5. Following insights from spectroscopy on binuclear Fe coordination complexes, this shift corresponds to a decrease of the Fe–O–Fe angle and hints to a considerable restructuring of such species. Moreover, the vibrational bands of isolated Fe species at 1010 and 1180 cm^{-1} for the calcined catalysts are replaced by one band at 1050 cm^{-1} upon high-temperature treatment. This indicates that the nature of the mononuclear species is also strongly modified. The dependence of the intensities of the various NO IR bands on the iron content is worthy of further discussion. The intensity of the band at 1874 cm^{-1} passes a maximum at Fe/Al = 0.66, whereas the intensity of the band around 1635 cm^{-1} decrease with iron content. These different trends are representative of the strong heterogeneity of the iron species in the high-temperature treated catalysts. The mixed iron and aluminum oxide species related to the band at 1874 cm^{-1} contains clustered iron species, while the mixed iron and aluminum oxide species characterized by the band at 1635 cm^{-1} might relate to a mononuclear Fe site. The combination of infrared and Raman spectroscopic data points to the presence of mononuclear Fe sites and oligonuclear sites in some interaction with extraframework Al species. The infrared spectra of adsorbed NO also reveal that the band intensities of nitro and nitrate groups on oligonuclear iron sites at 1625 and 1578 cm^{-1} in the Fe/ZSM-5(HT,x) catalysts are reduced as compared to the corresponding calcined catalysts. Their intensities increase with iron content. This result indicates that the amount of oligonuclear iron species that has not been altered during high-temperature treatment also increases with the iron content. These species are most probably small neutral iron oxide clusters in the micropores or at the external surface that do not interact with the zeolite anionic sites. The bands at 1912 and 1812 cm^{-1} due to poly-nitrosyl on isolated Fe species in the ten-membered rings of ZSM-5 are observed for both the calcined and the high-temperature treated Fe/ZSM-5(0.66) and Fe/ZSM-5(1.0) materials. These observations indicate that the nature of isolated iron species located in highly accessible positions in the zeolite micropores is hardly modified by the high-temperature treatment.

We envision the reconstruction of during high-temperature treatment as follows. High-temperature treatment will initially lead to more extensive interaction of the iron oxide particles with the anionic exchange sites of the zeolite as evidenced earlier by Zhu et al. [34]. In essence, this is a protolysis reaction of small iron oxide agglomerates. The severe conditions will further result in the removal of a considerable fraction of the tetrahedral framework Al species from the zeolite framework. The observation that upon rehydration no regeneration of bridging hydroxyl groups occurs suggests that the dealumination is ex-

tensive. This will lead to a more defective zeolite structure, and the resulting Fe species are then most likely stabilized by the extraframework Al species. Concomitant with these processes iron species undergo more easy auto-reduction to form various ferrous species. This tendency may very well be related to the more flexible nature of the newly formed oligonuclear Fe species.

4.2. Active sites for nitrous oxide decomposition

The reaction rate for the decomposition of nitrous oxide per Fe atom increases at low iron loading and passes through a maximum for Fe/ZSM-5(C,0.66). The apparent activation energy decreases with increasing iron content and levels off at higher iron loading. These observations suggest the contribution of various types of iron species for nitrous oxide decomposition. The high activation energy and the inferior activity at low iron loading are in agreement with the observation of Bell and co-workers [16]. With increasing iron clustering, the activation energy is lowered and the activity was substantially enhanced. Thus, more clustered iron sites are beneficial for nitrous oxide decomposition in line with recent reports [12,29]. However, extensive clustering of iron species at higher iron loading results in the formation of relatively inactive bulk iron oxides which consequently results in a decrease in the reaction rate expressed per Fe atom. The kinetic parameters cohere well with other data in literature [16,42,67]. A similar tendency with the metal loading was reported for Cu/ZSM-5 zeolites [69].

High-temperature treatment of the Fe/ZSM-5 leads to profound changes in the kinetic parameters. The apparent activation energy lies around 190 kJ/mol in agreement with literature values [67] and our characterization suggest the formation of a different active site. The high apparent activation energy is compensated by a high pre-exponential factor, which results in the remarkably high activity of these catalysts. The apparent activation energies does not depend on the iron loading which points to the uniform nature of the active sites. Indeed, the activity correlates strongly with the pre-exponential factor which includes the number of active sites. In a simplified kinetic analysis, the apparent pre-exponential factor A is the product of the number of sites multiplied by the kinetic pre-exponential factor which is the ratio of the partition functions of the transition state excluding that of the reaction coordinate and that of the ground state. Assuming that the rate of nitrous oxide decomposition is proportional to the active site density (Table 1), a pre-exponential factor of about 10^{13} s^{-1} is computed. Such a value points to a surface reaction as the rate-limiting step rather than a desorption reaction and tentatively, the migration and combination of oxygen over the surface may be the difficult process in the decomposition of nitrous oxide under these conditions, which is in line with our recent study on the chemistry of N_2O decomposition over high-temperature treated Fe/ZSM-5 [65]. Characterization of the high-temperature treated catalysts suggested the formation of isolated and oligonuclear Fe sites in close interaction to an aluminum oxide phase (*vide supra*). The increase in the nitrous oxide decomposition correlates well with the intensity of the band at 1874 cm^{-1} which is argued to be due to small Fe clusters in interaction with aluminum. Thus, in line with earlier reports [12,25,36] some clustering is important for nitrous oxide decomposition.

4.3. Active site for benzene hydroxylation with nitrous oxide

The catalytic role of iron species at extraframework positions for selective benzene oxidation to phenol with nitrous oxide as oxidant has been investigated in many recent studies [4–14]. For the calcined catalysts, the phenol productivity was found to be very low. An increase in iron content leads to a drastic decrease in the selectivities of benzene and nitrous oxide due to the full combustion of benzene. This notion agrees with recent works showing that Fe/ZSM-5 materials which were not severely treated are not favorable for phenol formation [6,8,9]. Thus, clustered iron species appear to contribute to the full combustion of the reactant benzene and the product phenol. High-temperature treatment dramatically enhances the phenol productivity, mainly by increasing the selectivities of benzene and nitrous oxide. The conversion of nitrous oxide and benzene decrease for the catalysts with higher iron content after high-temperature treatment. Earlier, it has been shown that the band around 1635 cm^{-1} is related to active sites for selective benzene oxidation [12]. Here, again good phenol productivity is only observed for the catalysts which show an appreciable band at 1636 cm^{-1}. Moreover, with increasing Fe content the phenol reaction rate decreases in line with the decrease of the intensity of this band (Fig. 3). Thus, this forms additional indications that a reconstructed mononuclear iron species stabilized by extraframework Al is the active site for selective benzene oxidation. Evidence for the proposed isolated iron species as active sites for selective benzene oxidation also followed from ESR spectroscopy with specific g-values of 6.0 and 5.6 [14]. Theoretical studies of benzene oxidation have thus far also focused on mononuclear iron sites [37,38].

The present study suggests that post-synthesized Fe/ZSM-5 materials prepared by ion exchange of the Brønsted acid protons with $FeCl_3$ are not optimal for benzene oxidation to phenol. Even at low iron loading (Fe/Al = 0.11), Raman spectroscopy is able to detect oligonuclear iron sites. It is indeed well-known that the $FeCl_3$ precursor is prone to the formation of clustered iron species in ZSM-5 and in essence in the vapor deposition of this precursor a dimer is deposited in the zeolite micropore space [29,35]. The decrease in the rate of phenol formation with increasing iron content for the high-temperature treated catalyst is mainly due to the decreases of the nitrous oxide selectivity and the conversion of benzene to non-selective products. This observation is more likely due to the increased relative amount of small neutral iron oxide clusters that have not been altered during high-temperature treatment, as reflected by the increase of the intensity of the infrared band at 1626 cm^{-1} with iron content (Fig. 3). The detrimental role of iron oxide cluster on phenol formation has been demonstrated for the calcined catalyst in this study and has also been suggested in recent literature [8,9].

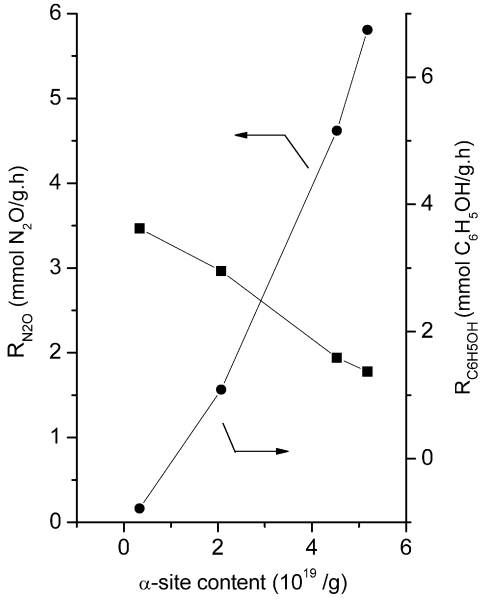

Fig. 11. Dependence of the rate of nitrous oxide decomposition at 693 K and rate of phenol formation at 623 K on the concentration of Fe^{2+} determined by CH_4 oxidation at room temperature.

4.4. Nature of active sites generated by high-temperature treatment

The activation of Fe-containing ZSM-5 zeolite under severe conditions leads to more active iron sites for decomposition of nitrous oxide and selective oxidation of benzene to phenol. Recently, several works [12,36] have provided insight into the relevance of extraframework Al species as an explanation for the necessity of the severe treatments. The present work provides some further insight into these issues. The spectroscopic data support considerable changes in the structure of mono- and oligonuclear Fe species upon high-temperature treatment and also point to the involvement of extraframework Al species. There is no direct proof that we are dealing with binuclear Fe species but it is clear that the nuclearity of these species is rather low. Relating spectroscopic data with the activity measurements provides strong evidence for the involvement of mononuclear sites in the selective benzene oxidation and of oligonuclear sites in catalytic nitrous oxide decomposition. Competing are the combustion reactions in benzene oxidation which also are catalyzed by more clustered Fe species. In general, these conclusions support earlier suppositions in literature [12] for isomorphously substituted FeZSM-5, by Sachtler and co-workers for benzene hydroxylation [6,7] and by Pérez-Ramírez et al. [21] for nitrous oxide decomposition.

Many authors agree with the notion that both reactions are catalyzed by Fe^{2+} sites generated upon severe treatment [4,37,38]. Fig. 11 displays the dependence of the rate of N_2O decomposition at 693 K and the rate of phenol formation at 623 K on the concentration of Fe^{2+} as determined by methane titration. The correlation strongly suggests that the Fe^{2+} species in the present series of Fe/ZSM-5 with an iron content in the range of 0.37–3.7 wt% catalyze mainly nitrous oxide decomposition. This discrepancy with earlier reports deserves some more discussion. First, it might be that oxidation with methane requires two surface oxygen in close proximity. This requirement might not be fulfilled for the mononuclear iron species. However, Dubkov et al. [43] have shown that even catalysts with surface oxygen concentration as low as 4×10^{18} g^{-1} can be probed by methane oxidation. For a Fe/ZSM-5 catalyst with an iron loading of 0.53 wt% the active site densities determined by titration by CO and CH_4 agreed well [51]. Hence, we exclude this possibility. Alternatively, it may be that, although titration by methane probes both mononuclear and binuclear iron species, the concentration of mononuclear sites is much lower than that of binuclear sites. Indeed, it is well-known that HZSM-5 zeolite with trace amounts of Fe are quite active in benzene oxidation [4]. Moreover, Hensen et al. [12] have shown that the amount of active sites involved in benzene oxidation is very low. In this regard, the volcano-type relation between the rate of phenol formation and the Fe^{2+} concentration as described by Panov and co-workers [13] is worthy of note. They changed the Fe^{2+} concentration by varying the iron loading and found that a linear correlation is only observed at very low iron loading (below 0.2 wt%). The rate of phenol formation will level off at medium Fe^{2+} concentration (at medium iron loading) and a further increase in Fe^{2+} concentration decreased the phenol formation. Indeed, if the relation observed for Hensen et al. [12] with iron loadings up to 0.6 wt% Fe and the present correlation (Fig. 11) with iron loading from 0.37 to 3.7 wt% are combined, a volcano-type correlation is found similar to the one reported by Panov and co-workers [13]. This volcano-type relation between the Fe^{2+} concentration and the rate of phenol formation can be interpreted in terms of two types of active sites. The linear increase in phenol formation with increasing Fe^{2+} concentration at very low iron loading is due to the increase of the density of mononuclear iron sites. The amount of oligonuclear sites at very low iron loading can be expected to be very low. Indeed, earlier work [12] has shown that the rate of catalytic nitrous oxide decomposition remains low at low loading and increases more than proportionally at higher iron loadings. The increase of the iron loading will result in the increase of the density of binuclear sites as revealed by Raman spectra (Fig. 6). This might be at the expense of the mononuclear sites explaining the decrease in the rate of phenol formation. Alternatively, it might also be that at higher iron contents several more clustered species contribute to secondary combustion reactions of phenol thus decreasing the selectivity. Conventionally, the active sites were thought to be cationic iron species stabilized at the anionic exchange sites of the zeolite [16,29,37,38]. However, our recent work has shown that even the introduction of extraframework Al to otherwise inactive iron-silicalite will not only favor the decomposition of nitrous oxide and the formation of Fe^{2+} sites [36], but also substantially promote the rate of phenol formation [10,11]. Those and the present findings strongly indicate the pivotal role of extraframework Al species in the formation of active sites. Taking into account the similar promotional role of extraframework Al species for these reactions, it appears that they facilitate the formation of highly active mono and oligonuclear iron sites. Another function may be to provide adsorption centers for the reactant.

5. Conclusion

A distribution of mononuclear and oligonuclear iron species in cationic exchange positions and more bulk iron oxide aggregates is observed in Fe/ZSM-5 after calcination at 823 K. An increase in the iron loading goes with increasing degree of iron clustering. High-temperature treatment results in the reconstruction of the cationic iron species. Vibrational spectroscopies evidence two kinds of new Fe species: mononuclear iron species were formed at the lowest iron loadings and clustered iron species of low nuclearity were identified for catalysts with an intermediate iron loading. These iron species are stabilized by extraframework Al in the micropores of the zeolite matrix. Estimation of the concentration of Fe^{2+} by low-temperature N_2O decomposition and by CH_4 titration reveals that the ferrous sites are mainly associated with the reconstructed oligonuclear iron site. Most likely, the concentration of mononuclear sites is very low in the present set of catalysts.

Nitrous oxide decomposition is favored at medium iron loading for both the calcined and high-temperature pretreated catalysts. The rate of nitrous oxide decomposition is about three times higher for Fe/ZSM-5 treated at high temperature. A strong correlation is identified between the rate of nitrous oxide decomposition and the presence of oligonuclear Fe species. The oligonuclear Fe species stabilized by extraframework Al formed as result of high-temperature treatment of Fe/ZSM-5 are the most favorable sites for nitrous oxide decomposition. For benzene hydroxylation to phenol, the calcined samples show negligible activity. High-temperature treatment improves the activity and selectivity. Nevertheless, the rate of phenol formation decreases strongly with increasing iron loading. It is argued that mononuclear sites are active in the selective oxidation reaction.

Acknowledgments

This work is financially supported by the Programme for Strategic Scientific Alliances between China and Netherlands (grant No. 2004CB720607, NSFC grant No. 20520130214, Grant No. 04-PSA-M-01) and the National Basic Research Program of China (grant Nos. 2003CB615806, 2005CB221407) and the National Natural Science Foundation of China (grant Nos. 20773118, 20673115).

References

[1] G. Centi, S. Perathoner, F. Vanazza, M. Marella, M. Tomaselli, M. Mantegazza, Adv. Environ. Res. 4 (2000) 325.
[2] J. Pérez-Ramírez, F. Kapteijn, G. Mul, J.A. Moulijn, Chem. Commun. (2001) 693.
[3] J. Pérez-Ramírez, F. Kapteijn, G. Mul, J.A. Moulijn, Appl. Catal. B 35 (2002) 227.
[4] G.I. Panov, Cattech 4 (2000) 18.
[5] G.I. Panov, V.I. Sobolev, A.S. Kharitonov, J. Mol. Catal. 61 (1990) 85.
[6] J. Jia, K.S. Pillai, W.M.H. Sachtler, J. Catal. 221 (2004) 119.
[7] K.S. Pillai, J. Jia, W.M.H. Sachtler, J. Catal. 264 (2004) 133.
[8] E.J.M. Hensen, Q. Zhu, M.M.R.M. Hendrix, A.R. Overweg, P.J. Kooyman, M.V. Sychev, R.A. van Santen, J. Catal. 221 (2004) 575.
[9] I. Yuranov, D.A. Bulushev, A. Renken, L. Kiwi-Minsker, J. Catal. 227 (2004) 138.
[10] E.J.M. Hensen, Q. Zhu, R.A. van Santen, J. Catal. 220 (2003) 260.
[11] E.J.M. Hensen, Q. Zhu, R.A.J. Janssen, P.C.M.M. Magusin, P.J. Kooyman, R.A. van Santen, J. Catal. 233 (2005) 123.
[12] E.J.M. Hensen, Q. Zhu, R.A. van Santen, J. Catal. 233 (2005) 136.
[13] L.V. Pirutko, V.S. Chernyavsky, A.K. Uriarte, G.I. Panov, Appl. Catal. 227 (2002) 143.
[14] P. Kubánek, B. Wichterlová, Z. Sobalík, J. Catal. 211 (2002) 109.
[15] X. Feng, W.K. Hall, J. Catal. 166 (1997) 368.
[16] H.-Y. Chen, W.M.H. Sachtler, Catal. Today 42 (1998) 73.
[17] R. Joyner, M. Stockenhuber, J. Phys. Chem. B 103 (1999) 5963.
[18] R.Q. Long, R.T. Yang, J. Am. Chem. Soc. 121 (1999) 5595.
[19] M. Uddin, T. Komatsu, T. Kashima, J. Catal. 150 (1994) 439.
[20] R.Q. Long, R.T. Yang, Chem. Commun. (2000) 1651.
[21] J. Pérez-Ramírez, F. Kapteijn, G. Mul, J. Moulijn, J. Catal. 208 (2002) 211.
[22] E.J.M. Hensen, Q. Zhu, M.M.R.M. Hendrix, A.R. Overweg, P.J. Kooyman, M.V. Sychev, R.A. van Santen, J. Catal. 221 (2004) 560.
[23] L.J. Lobree, I.C. Hwang, J.A. Reimer, A.T. Bell, J. Catal. 186 (1999) 242.
[24] P. Fejes, K. Lázár, I. Marsi, A. Rockenbauer, L. Korecz, J.B. Nagy, S. Perathoner, G. Centi, Appl. Catal. A Gen. 252 (2003) 75.
[25] J. Pérez-Ramírez, G. Mul, F. Kapteijn, J.A. Moulijn, A.R. Overweg, A. Doménech, A. Ribera, I.W.C.E. Arends, J. Catal. 207 (2002) 113.
[26] P. Marturano, L. Drozdova, A. Kogelbauer, R. Prins, J. Catal. 192 (2000) 236.
[27] M.S. Kumar, M. Schwidder, W. Grunert, A. Brückner, J. Catal. 227 (2004) 384.
[28] G. Berlier, G. Spoto, S. Bordiga, G. Ricchiardi, P. Fisicaro, A. Zecchina, I. Rossetti, E. Selli, L. Forni, E. Giamello, C. Lamberti, J. Catal. 208 (2002) 64.
[29] P. Marturano, L. Drozdova, G.D. Pirngruber, A. Kogelbauer, R. Prins, Phys. Chem. Chem. Phys. 3 (2001) 5585.
[30] S. Bordiga, R. Buzzoni, F. Geobaldo, C. Lamberti, E. Giamello, A. Zecchina, G. Leofanti, G. Petrini, G. Tozzola, G. Vlaic, J. Catal. 158 (1996) 486.
[31] G. Mul, J. Pérez-Ramírez, F. Kapteijn, J. Moulijn, Catal. Lett. 80 (2002) 129.
[32] H.-Y. Chen, E.M. Malki, X. Wang, R.A. van Santen, W.M.H. Sachtler, J. Mol. Catal. A Chem. 162 (2000) 159.
[33] Z.-X. Gao, H.-S. Kim, Q. Sun, P.C. Stair, W.M.H. Sachtler, J. Phys. Chem. B 105 (2001) 6186.
[34] Q. Zhu, E.J.M. Hensen, B.L. Mojet, J.H.M.C. van Wolput, R.A. van Santen, Chem. Commun. (2002) 1232.
[35] A.A. Battison, J.H. Bitter, F.M.F. de Groot, A.R. Overweg, O. Stephan, J.A. van Bokhoven, P.J. Kooyman, C. van de Spek, G. Vankó, D.C. Koningsberger, J. Catal. 213 (2003) 251.
[36] K. Sun, H. Zhang, H. Xia, Y. Lian, Y. Li, Z. Chi, P. Ying, C. Li, Chem. Commun. (2004) 2480.
[37] J.A. Ryder, A.K. Chakraborty, A.T. Bell, J. Catal. 220 (2003) 84.
[38] N.A. Kachurovskaya, G.M. Zhidomirov, R.A. van Santen, J. Phys. Chem. B 108 (2004) 5944.
[39] L.M. Kustov, A.L. Tarasov, V.I. Bogdan, A.A. Tyrlov, J.W. Fulmer, Catal. Today 61 (2000) 123.
[40] J.L. Motz, H. Heinichen, W.F. Hölderich, J. Mol. Catal. 136 (1998) 175.
[41] G.I. Panov, A.K. Uriarte, M.A. Rodkin, V.I. Sobolev, Catal. Today 41 (1998) 365.
[42] Q. Zhu, B.L. Mojet, R.A.J. Janssen, E.J.M. Hensen, J. van Grondelle, P.C.M.M. Magusin, R.A. van Santen, Catal. Lett. 81 (2002) 205.
[43] R. Burch, C. Howitt, Appl. Catal. A 103 (1993) 135.
[44] V.L. Zholobenko, I.N. Senchenya, L.M. Kustov, V.B. Kazansky, Kinet. Catal. 32 (1991) 151.
[45] J.L. Motz, H. Heinrichen, W.F. Hölderich, J. Mol. Catal. 136 (1998) 175.
[46] L.M. Kustov, A.L. Tarasov, V.I. Bogdan, A.A. Tyrlov, J.W. Fulmer, Catal. Today 61 (2000) 123.
[47] P.M. Esteves, B. Louis, J. Phys. Chem. B 110 (2006) 16793.
[48] K.A. Dubkov, N.S. Ovanesyan, A.A. Shteinman, E.V. Starokon, G.I. Panov, J. Catal. 207 (2002) 341.
[49] B. Sulikowski, J. Find, H.G. Karge, D. Herein, Zeolites 19 (1997) 395.
[50] L. Kiwi-Minsker, D.A. Bulushev, A. Renken, J. Catal. 219 (2003) 273.

[51] K.A. Dubkov, E.A. Paukshtis, G.I. Panov, Kinet. Catal. 42 (2001) 205.
[52] P.O. Fritz, J.H. Lunsford, J. Catal. 118 (1989) 85.
[53] L.J. Lobree, I.C. Hwang, J.A. Reimer, A.T. Bell, Catal. Lett. 63 (1999) 233.
[54] G. Spoto, A. Zecchina, G. Berlier, S. Bordiga, M.G. Clerici, L. Bisini, J. Mol. Catal. A Chem. 158 (2000) 107.
[55] J. Pérez-Ramírez, F. Kapteijn, A. Brückner, J. Catal. 214 (2003) 33.
[56] L. Čapek, V. Kreibich, J. Dědeček, P. Grygar, B. Wichterlová, Z. Sobalík, J.A. Martens, R. Brosius, V. Tokarivá, Microporous Mesoporous Mater. 80 (2005) 279.
[57] G.D. Pirngruber, P.K. Roy, R. Prins, Phys. Chem. Chem. Phys. 8 (2006) 3939.
[58] C. Li, J. Catal. 216 (2003) 203.
[59] R.J. Thibeau, C.W. Brown, R.H. Heidersbach, Appl. Spectrosc. 32 (1978) 532.
[60] A.J.M. De Man, J. Phys. Chem. 100 (1996) 5025.
[61] C. Li, G. Xiong, Q. Xin, J.-K. Liu, P.-L. Ying, Z.-C. Feng, J. Li, W.-B. Yang, Y.-Z. Yang, G.-R. Wang, X.-Y. Liu, M. Lin, X.-O. Wang, W.-Z. Min, Angew. Chem. Int. Ed. 28 (1999) 2220.
[62] L. Que Jr., W.B. Tolman, Angew. Chem. Int. Ed. 41 (2002) 1114.
[63] D.M. Kurtz Jr., Chem. Rev. 90 (1990) 585.
[64] J. Jia, B. Wen, W.M.H. Sachtler, J. Catal. 210 (2002) 453.
[65] K.-Q. Sun, H. Xia, E.J.M. Hensen, R.A. van Santen, C. Li, J. Catal. 238 (2006) 186.
[66] B.R. Wood, J.A. Reimer, A.T. Bell, J. Catal. 209 (2002) 151.
[67] P.K. Roy, G.D. Pirngruber, J. Catal. 227 (2003) 164.
[68] B.R. Wood, J.A. Reimer, A.T. Bell, M.T. Janicke, K.C. Ott, J. Catal. 224 (2004) 148.
[69] P.J. Smeets, M.H. Groothaert, R.M. van Teeffelen, H. Leerman, E.J.M. Hensen, R.A. Schoonheydt, J. Catal. 245 (2007) 358.